

# Experimental report

21/10/2022

**Proposal:** 5-53-296

**Council:** 4/2020

**Title:** Search for Loop currents in two-leg CuO ladders at high Ca-doping

**Research area:** Physics

**This proposal is a resubmission of 5-53-292**

**Main proposer:** Dalila BOUNOUA

**Experimental team:** Lucile MANGIN-THRO  
Dalila BOUNOUA

**Local contacts:** Lucile MANGIN-THRO

**Samples:** Sr<sub>2</sub>Ca<sub>12</sub>Cu<sub>24</sub>O<sub>41</sub>

Instrument	Requested days	Allocated days	From	To
D7	8	8	22/02/2021	02/03/2021

## Abstract:

We discovered the existence of a new kind of short-range magnetism in the two-leg ladder (Sr,Ca)<sub>14</sub>Cu<sub>24</sub>O<sub>41</sub> family of cuprates [1]. Observed for the Ca contents  $x = 5$  and  $8$ , this magnetism develops within the two-leg ladders and exhibits increasing correlations with increasing hole-doping. Its magnetic scattering further displays a very specific momentum dependence, the hallmark of a theoretically predicted loop current magnetism in such a material [2, 3]. Our discovery brings a novel insight onto the nature of the magnetic properties of hole-doped two-leg ladder cuprates and suggests that a loop current phase could act as a precursor to the S =  $\frac{1}{2}$  antiferromagnetic state at larger Ca content. We want to complement our study and probe the interplay between this novel magnetic phase and the AF-LRO state in a highly doped compound ( $x_{Ca}=12$ ). To this aim, we ask for 8 days on D7.

# Search for loop currents in a two leg ladder-cuprate

The family of the two-leg spin  $\frac{1}{2}$  ladder cuprates  $\text{Sr}_{(14-x)}\text{Ca}_x\text{Cu}_{24}\text{O}_{41}$  (hereafter: SCCO-x) has attracted a lot of interest, owing to the emergence of superconductivity upon substitution [4]. The Ca-free compound  $\text{Sr}_{14}\text{Cu}_{24}\text{O}_{41}$  is a quasi-1D system, which consists of two interpenetrating subsystems of  $\text{CuO}_2$  chains and  $\text{Cu}_2\text{O}_3$  two-leg ladders. It realizes an intrinsically hole-doped compound with an effective charge of  $+2.25$  per Cu (mixed valence  $\text{Cu}_{2+/3+}$ ), where the holes are located within the chains subsystem. Substitution with  $\text{Ca}_{2+}$  on the  $\text{Sr}_{2+}$  site results in a transfer of the holes carriers from the chains to the ladders subsystem [5]. Ca-doping results in a rich P-T phase diagram with various phases: spin liquid state, antiferromagnetic state, charge density wave, superconductivity under pressure [6]. A long-range ordered antiferromagnetic (AF-LRO) phase was also reported for  $x \geq 9$ . The origin of the AF-LRO is however still unclear. Indeed, while it was attributed to AF ordering within the chains, it was also proposed to originate from AF spin ordering within the ladders [7-8]. To account for such an AF state, one needs to elaborate a very complex magnetic pattern made of a large number of Cu spins.

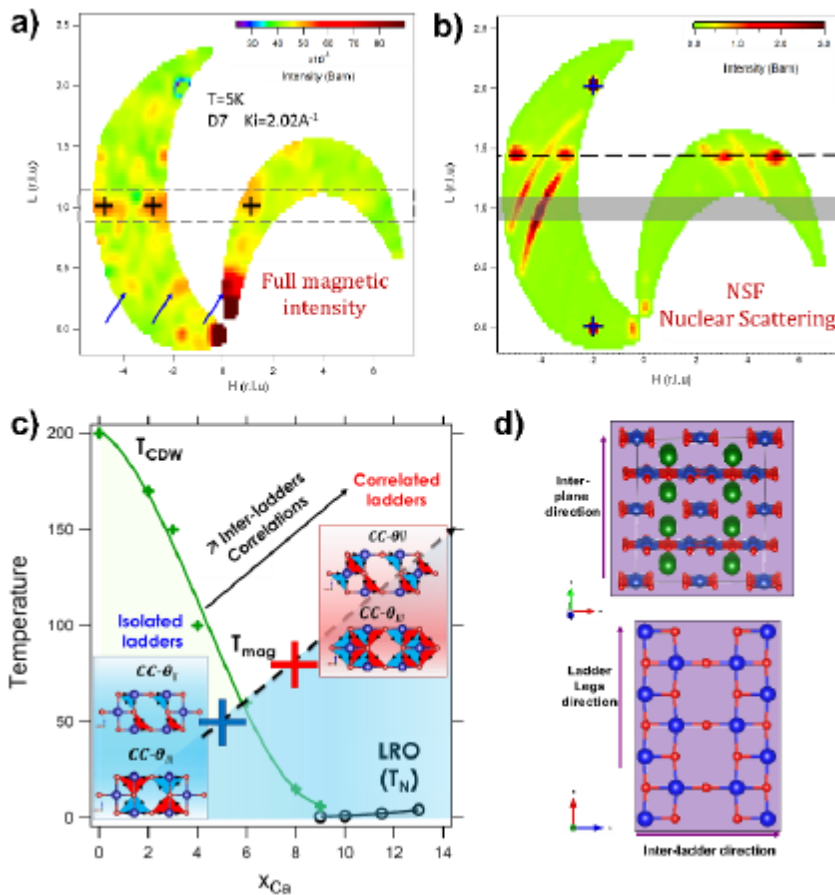
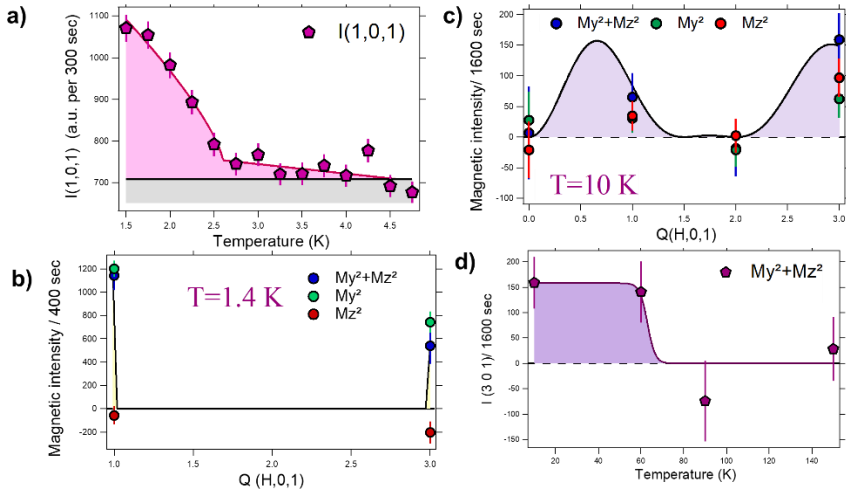


Figure 1 (a) SCCO-8: Mapping of the full magnetic scattering at 5K, deduced from XYZ-PA on D7. The map is given in r.l.u. of the ladders subsystem and the intensities in mbarn. The area bounded by dashed lines indicates the ladder scattering ridge along  $(H, 0, 1)$  with magnetic spots located by crosses. The blue arrows show the satellite magnetic reflections. (b) SCCO-8: Mapping of nuclear intensity measured in the NSF channel. Spots at integer  $H$  and  $L$  values correspond to the nuclear scattering associated with the ladders, whereas the dashed lines are associated with the chains nuclear response. (c) Schematic phase diagram showing the evolution of the LC pattern as a function of the hole-doping (i.e. Ca-content). At large doping, inter-ladders correlations set-in and  $T_{\text{mag}}$  (crosses) increases. In heavily doped samples, an AFM-LRO further develops below  $T_N$  of a few Kelvin. Insets: (Up) CC-II like model of LCs within one ladder unit cell with two staggered Cu-O orbital currents per Cu site flowing clockwise (red triangles) and anticlockwise (blue triangles). (Down) CC-III model of LCs, as derived from a spin liquid initial state [3], within the ladder cell consisting of two counter-propagating currents flowing between oxygen sites. (d) Up: Crystal structure of SCCO (Cu in blue, O in red and Sr in green). Down:  $[a, c]$  plane projection of the ladders planes.

We have revisited the magnetic properties of SCCO-x, using polarized neutron diffraction (PND) [1]. Our PND measurements in two different SCCO single crystals with Ca doping levels  $x=5$  and 8, using two different instruments (The cold-TAS 4F1 and the multi-detector diffractometer D7), equipped with distinct neutron polarization set-ups and operating with 2 distinct neutron wavelengths ( $k_i=2.57 \text{ \AA}^{-1}$  for 4F1 and  $k_i=2.02 \text{ \AA}^{-1}$  for D7). For both samples, PND measurements show the onset of a new magnetism. This one is at short range and preserves the lattice translational invariance ( $\mathbf{q}=0$  magnetism). It further gives rise to scattering on top of Q-positions where no nuclear scattering is expected from space-group symmetry selection rules [9] (Fig.1.a.b). The characteristic onset temperature for the magnetic correlations was found to be  $T_{\text{mag}}=50\text{K}$  and  $80\text{K}$  for SCCO-5 and SCCO-8 (Fig.1.c), respectively. At low Ca content, only the magnetic response of one single isolated ladder is measured (SCCO-5:  $\xi_c \sim 20 \text{ \AA}$ , along the ladders legs and no correlation along  $a$ , the ladders rungs, Fig.1.d), Increasing the Ca content, SCCO-8 exhibits finite correlations along both the  $a$  and  $c$ -axis ( $\xi_c \sim 11 \text{ \AA}$  and  $\xi_a \sim 6 \text{ \AA}$ ). For both compounds, no magnetic correlations were found along the inter-plane direction (b-axis, Fig.1.d). The corresponding Q-dependence of the magnetic intensity along  $(H, 0, 1)$  can be accounted for by an orbital magnetism produced by staggered loop currents (LCs) within the  $\text{CuO}_2$  plaquettes of 2 leg-ladders [2,3]. The result reminds the observation of loop currents confined in charged stripes ladders in lightly doped  $\text{La}_{2-x}\text{Sr}_x\text{CuO}_4$  [10]. While LCs are expected to be absent in hole free ladders, they progressively develop upon hole doping [2,11]. Modeling our data by using two different patterns of LCs nicely captures the main features of our experimental results and give a very small amplitude for the corresponding magnetic moment ( $m \sim 0.05 \mu_B$ ).

Our measurements further pinpoint the increase of correlation lengths upon increasing the Ca-content, going along with the development of a magnetic LRO at high Ca-doping. Besides, the LC-like  $q=0$  magnetism appears on Q-positions where scattering from LRO was reported using PND [7-8]. However, no LRO is reported for SCCO-5 and 8,  $T_{\text{mag}} \gg T_N$  (Fig.1.c).

A pilot experiment on the TAS-IN22 (Exp **CRG-2614**, Fig.2) allowed us to confirm the persistence of such a LCs phase in a  $x=12$  SCCO compound where LRO occurs at low temperatures, with a magnetic moment orientation specific to each phase. For  $x_{\text{Ca}}=12$ , the ordering temperature is found to be  $T=2.7\text{K}$  as measured by neutron diffraction (Fig 2.a-b), consistent with earlier works in literature [12].



**FIG. 2:** SCCO-12. (a) Temperature dependence of the intensity at the magnetic Bragg peak  $(1,0,1)$  giving  $T_N = 2.7\text{K}$ . The grey area is the background value estimated from a longitudinal scan, collected at  $1.4\text{K}$  (b) XYZ-PA of the magnetic scattering along the  $(H,0,1)$  line in the LRO-phase at  $T=1.4\text{K}$ . The data show a very weak, if any, out-of-plane contribution  $M_z^2$  to magnetic scattering as compared to  $My^2$  (c) XYZ-PA along the  $(H,0,1)$  scattering line of the ladders subsystem. The solid bold line is a fit to the data using a  $CC-\Theta_{ij}$  like model of LCs within the ladders [2-3]. The XYZ-PA shows that the measured magnetic moments includes both an in-plane  $M_y$  and out-of-plane  $M_z$  components. (d) Temperature dependence of the magnetic signal extracted from XYZ-PA at  $(3,0,1)$  at few key temperatures. The fits to the data gives an approximate  $T_{\text{mag}} = 65\text{K}$ . The data were collected on the TAS IN22,  $ki=2.662\text{\AA}^{-1}$ .

### Experiment # 5-53-296:

The objective of the experiment was to map the Q-dependence of the LCs like magnetism in the highly Ca-doped  $\text{Sr}_2\text{Ca}_{12}\text{Cu}_{24}\text{O}_{41}$ . The sample consisted in a single crystal grown by the travelling solvent floating zone method of  $\sim 1\text{g}$  total weight (Similar to  $\text{Sr}_6\text{Ca}_8\text{Cu}_{24}\text{O}_{41}$  used in experiment #5-53-279). The sample was aligned in  $[a,c]$  plane of the ladders subsystem. A full rocking scan of  $360^\circ$  was first performed to check the alignment of the sample at  $5\text{K}$ . Reflections of the form  $(H00)$  and  $(00L_cL_l)$  where  $L_c$  and  $L_l$  correspond to the chains and ladders, respectively. The aim was to search for a magnetic signal occurring at positions of the form  $(H,0,1)$  with  $L_c=1$  and  $H=1$  or  $3$  corresponding to the ladders subsystem and where a new magnetic signal was reported in Ca-doped samples. Omega scans were performed using XYZ-PA first spanning a large portion of reciprocal space including both  $(-1,0,1)$  and  $(-3,0,1)$  Q-points. The study was performed with a wavelength  $\lambda=3.1$  and for two values of  $2\theta$ , namely,  $75.5$  and  $80^\circ$  in order to fully fill the dead zones corresponding to the hollow regions between detectors. The measurements were carried at both  $T=300\text{K}$  and  $T=7\text{K}$  (above the magnetic ordering temperature).

### Results from NSF measurements at low temperature:

Figure 3 shows and NSFx map of the intensity at  $T=7\text{K}$  indicating nuclear scattering arising from the ladders subsystem  $(H,0,L)$  with  $H+L$  even and  $L$  integer and the chains subsystem  $(H,0,1.43)$ .

The  $(H,0,0)$  line corresponds to combined scattering from the chains and ladders lattices occurring at even  $H$  values. The circular halos are due to powder scattering from the Al sample holder. One can notice that nuclear scattering occurs on the  $(H,0,1)$  line as far as  $H+L$  is even. This is to contract with the case of SSCO-5 and 8 compounds where the space group selection rules were different ( $H$  and  $L$  even) and no scattering occurred at  $(H,0,1)$  positions.

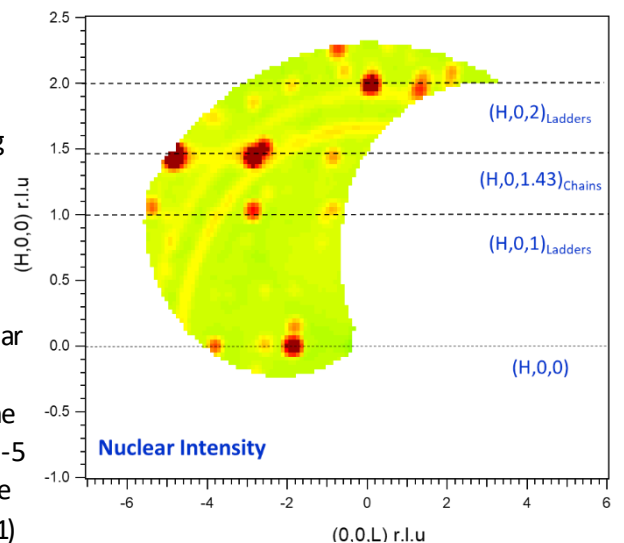


**Figure 3:** NSFx map collected at  $T=5\text{K}$

## Results from XYZ-PA measurements at low temperature:

Figure 4.a shows the resulting magnetic intensity at  $T=7\text{K}$  ( $2^*SF_x-SF_y-SF_z$ , corrected by an angle  $\alpha=41.6^\circ$  corresponding to the angle between  $X$  and  $k_i$ ). The map was obtained by collecting data at a large number of omega values (132 in total) to span both  $(-1,0,1)$  and  $(-3,0,1)$ . The polarization imperfections were corrected using a quartz sample and the intensity converted to absolute units using a vanadium reference sample.

The map shows the occurrence of scattering at  $(-3,0,1)$  as expected for the magnetic signal from our previous measurements. Owing to the presence of nuclear scattering at  $(-3,0,1)$  arising from a change of the space group selection rules when moving from low to high Ca-doping samples, and in order to rule out simple polarization leakage from the NSF to the SF channel giving fictitious magnetic scattering, we analyzed the FWHM and temperature dependence of the signal.

Fig.4.b-c show typical H-scans along the  $(-3,0,L)$  line around  $L=1$ , extracted from both XYZ-PA and  $NSF_x$  data at  $7\text{K}$ . The typical FWHM of the peak on Fig.3.b is  $0.08\pm 0.02$ , larger than the one of the nuclear Bragg peak at  $(3,0,1)$   $0.041\pm 0.001$  r.l.u, consistent with previous measurements on IN22, confirming its magnetic nature and ruling out spurious scattering due to polarization leakage.

In order to crosscheck that, we repeated the same measurement at  $300\text{K}$ . The data are shown on Fig.4.c and confirm the disappearance of the magnetic signal upon heating.

Other “hot spots” on Fig.4.a at  $(-2,0,0)$  and  $(-3,0,1.43)$  are due to polarization leakage from the NSF to the SF channel as checked from the corresponding FWHM of the Bragg peaks and their persistence up to high temperature.

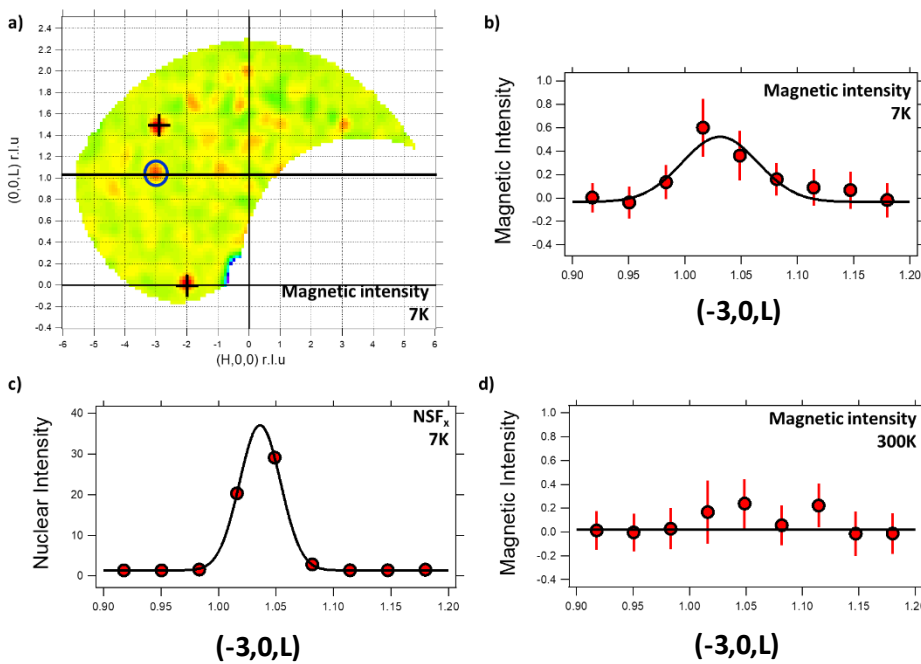


**Figure 4:** a) Full magnetic intensity as extracted from XYZ-PA at  $T=7\text{K}$ . b) L-scan along  $(-3,0,L)$  obtained by XYZ-PA at  $7\text{K}$ . c) L-scan along  $(-3,0,L)$  obtained in the  $NSF_x$  channel. d) L-scan along  $(-3,0,L)$  obtained by XYZ-PA at  $300\text{K}$ .

## References

- [1] D. Bounoua et al *Commun Phys* 3, 123 (2020).
- [2] C. M. Varma. *Phys. Rev. B* 73, 155113 (2006).
- [3] S. Scheurer et al., *Phys. Rev. B* 98(23), 235126 (2018).
- [4] M. Uehara et al., *J. Phys. Soc. Jpn.*, 65(9), 2764 (1996).
- [5] Y. Gotoh et al., *Phys. Rev. B* 68, 224108 (2003).
- [6] T. Vuletic, et al., *J. Phys. Rep.* 428(4), 169–258 (2006).
- [7] M. Isobe, M et al., *Phys. Rev. B* 59(13), 8703 (1999).
- [8] G. Deng, et al., *Phys. Rev. B* 88(17), 174424 (2013).

- [9]  $\text{Sr}_{14}\text{Cu}_{24}\text{O}_{41}$  crystallizes in an orthorhombic structure (Fig.1.e) The chains and ladders subsystems are described by the orthorhombic space groups  $Amma$  and  $Fmmm$ , respectively, that interpenetrate incommensurately along the  $c$ -axis with  $10^*c_{\text{Chains}}=7^*c_{\text{Ladders}}$ . Upon Ca doping, the chains sub-space group changes from  $Amma$  to  $Fmmm$  such that the whole structure was described by Deng et al., as belonging to  $Xmmm(00g)ssO$  superspace group.
- [10] V. Balédent et al., *Phys. Rev. Lett.* 105, 027004 (2010).
- [11] P. Chudzinski et al., *Phys. Rev. B* 76, 161101(R) (2007); *Phys. Rev. B* 78, 075124 (2008); and *Phys. Rev. B* 81, 165402 (2010).
- [12] M. Nagata et al., *J. Phys. Soc. Jpn.* 68(7), 2206–2209 (1999).